Climatic Change (2010) 98:277–284
DOI 10.1007/s10584-009-9758-0

LETTER

Changes in European temperature extremes can be predicted from changes in PDF central statistics

A letter

Joan Ballester · Filippo Giorgi · Xavier Rodó

Received: 12 August 2009 / Accepted: 16 October 2009 / Published online: 11 November 2009

Abstract Although uncertainties are still large, many potentially dangerous effects have already been identified concerning the impacts of global warming on human societies. For example, the record-breaking 2003 summer heat wave in Europe has given a glimpse of possible future European climate conditions. Here we use an ensemble of regional climate simulations for the end of the twentieth and twenty-first centuries over Europe to show that frequency, length and intensity changes in warm and cold temperature extremes can be derived to a close approximation from the knowledge of changes in three central statistics, the mean, standard deviation and skewness of the Probability Distribution Function, for which current climate models are better suited. In particular, the effect of the skewness parameter appears to be crucial, especially in the case of cold extremes, since it mostly explains the relative warming of these events compared to the whole distribution. An application of this finding is that the future impacts of extreme heat waves and cold spells on non-climatological variables (e.g., mortality) can be estimated to a first-order approximation from observed time series of daily temperature transformed in order to account for simulated changes in these three statistics.

Electronic supplementary material The online version of this article (doi:10.1007/s10584-009-9758-0) contains supplementary material, which is available to authorized users.

J. Ballester (✉) · X. Rodó
Institut Català de Ciències del Clima (IC3), Carrer Dr. Trueta 203,
08005 Barcelona, Catalonia, Spain
e-mail: joanballester@ic3.cat

F. Giorgi
Abdus Salam International Centre for Theoretical Physics, Trieste, Italy

1 Introduction

The increase in atmospheric greenhouse gas concentrations has led to a detectable anthropogenically induced global warming since the mid twentieth century (IPCC 2007). Climate model projections indicate that mean temperature rise will generate a range of global and local impacts in many natural and human systems (Rodó et al. 2002; Parmesan and Yohe 2003). In particular, the European region emerges as an especially responsive area to global warming (Ballester et al. 2009a), particularly during the warm season (Giorgi 2006). In its latest report, the IPCC pointed out that there is an increasing concern about temperature warm extremes, which are expected to become more frequent, longer and more severe (Meehl and Tebaldi 2004). Conversely, although only a few studies have addressed the issue of cold spells (IPCC 2007), they are expected to decrease mainly as a result of the mean annual warming (Ballester et al. 2009a).

The resolution of current Coupled Atmosphere-Ocean General Circulation Models (AOGCMs) reaches about 150 km at major modeling centers. To complement the AOGCM information, Regional Climate Models (RCMs) can be applied to climate change studies to produce fine scale regional information, with a grid resolution of tens of km (Giorgi and Mearns 1999). In particular, RCMs have been shown to improve the simulation of extreme events compared to coarser resolution models (Giorgi and Mearns 1999). The European project PRUDENCE (Christensen et al. 2007, see references therein) represents probably the most advanced application of RCMs in the literature, whereby an ensemble of regional models was used to produce high resolution (∼50 km) climate change projections over Europe for different scenarios and driving AOGCMs.

Here we compute scenario changes (1961–1990 versus B2 or A2 2071–2100 (IPCC 2007)) in the warm and cold extreme tails of European daily Maximum (TMAX), Mean (TMEAN) and Minimum (TMIN) 2-m Temperatures. Simulations for the B2 (A2) scenario are based on an ensemble of six (ten) RCMs from the PRUDENCE project (Ballester et al. 2009b). Using a simple methodology, the detrended control simulation (CTL) time series is transformed so that it has the same mean and/or standard deviation and/or skewness as the detrended scenario simulation (SCE). The resulting temperature time series defines new artificially-created synthetic scenarios (Section 2), and their ability to reproduce future changes in both the warm and cold Probability Distribution Function (PDF) tails for the original scenario simulation is evaluated (Section 3). Results and their applications are then discussed (Section 4).

2 Methods

The hypothesis tested in this article is whether expected changes in the temperature PDF tails can be basically reproduced by changes in the mean (μ), standard deviation (σ) and/or skewness (*skw*) of the PDF, where the PDF refers to the full distribution of daily temperatures throughout the year. Projected anomalies in these three statistics from the PRUDENCE ensemble for the European region are shown in Fig. 1. Positive anomalies in the mean, standard deviation and skewness indicate that annual mean temperatures shift to warmer values, the PDF widens (as a result for

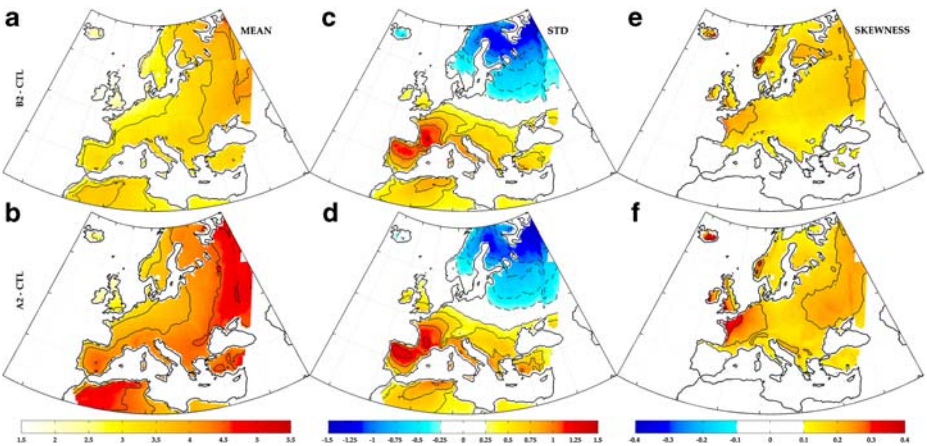

Fig. 1 Forecasted multi-model ensemble mean scenario changes (scenario-control) in detrended daily TMEAN (K). B2 (**a**, **c**, **e**) and A2 (**b**, **d**, **f**) scenario anomalies correspond to the PDF mean (**a**, **b**), standard deviation (**c**, **d**) and skewness coefficient (**e**, **f**), respectively

example of an intensification of the seasonal cycle (Ballester et al. 2009b)) and both extreme tails warm to a larger degree than central percentiles, respectively.

Different synthetic scenarios are then derived from local detrended CTL time series in which the mean, standard deviation and/or skewness coefficient of the PDF are readjusted to attain the values of these three central statistics as inferred from a simulated future scenario (here, B2 or A2) time series. In other words, the detrended daily CTL time series is assigned to these synthetic scenarios, but it is transformed so that its mean, standard deviation and/or skewness coefficient equal those of the detrended B2 or A2 time series. Note that in this transformation nothing except the mean, standard deviation and/or skewness is used from the B2 or A2 local time series, so that the new synthetic scenario is derived only from the CTL simulation and the three central statistics in the B2 or A2 simulation. Specific information about future extremes (frequency, intensity, length or distribution of extremes) is therefore not used in the construction of these synthetic scenarios. Please, find the complete description of the transformation in the Supplementary Material.

Results are here shown for three types of artificially-created synthetic scenarios, which we name M, MS, and MSW, for both the B2 and A2 IPCC scenarios. They are defined as:

1. M-B2 (or M-A2): for each grid-point and model, the local time series $f(x)$ in the new synthetic scenario is equal to the local CTL time series x, but its mean is shifted to the mean value of the B2 (or A2) local time series y, i.e.,

$$\mu(f(x)) = \mu(y),\ \sigma(f(x)) = \sigma(x),\ skw(f(x)) = skw(x),\ \text{and}\ corr(x,\ f(x)) = 1.$$

2. MS-B2 (or MS-A2): the local CTL time series x is transformed into the local time series $f(x)$ in the new synthetic scenario, so that it has the same mean and standard deviation as the B2 (or A2) local time series y, i.e.,

$$\mu(f(x)) = \mu(y),\ \sigma(f(x)) = \sigma(y),\ skw(f(x)) = skw(x),\ \text{and}\ corr(x,\ f(x)) = 1.$$

3. MSW-B2 (or MSW-A2): all the three central statistics for the local time series $f(x)$ in the new synthetic scenario are equal to those in the B2 (or A2) local time series y, i.e.,

$$\mu\,(f\,(x)) = \mu\,(y)\,,\ \sigma\,(f\,(x)) = \sigma\,(y)\,,\ skw\,(f\,(x)) = skw\,(y)\,,\ \text{and almost always}\ corr\,(x,\ f\,(x)) \approx 1.$$

In the present work, we also define as central cold (warm) temperatures the range of percentiles within $P10 \leq T \leq P50\,(P50 \leq T \leq P90)$, and the extreme cold (warm) tail as those values within $P0.1 \leq T \leq P1\,(P99 \leq T \leq P99.9)$.

3 Results

In a first attempt to describe changes in both temperature PDF tails by means of changes in either one or more of the three central statistics, the ability of synthetic scenarios to reproduce expected changes is evaluated for the frequency of tail days and the length of tail events. For each grid-point and model, a warm (cold) tail day in CTL and in an original or artificial scenario simulation is defined as a day above (below) a given temperature percentile of CTL, and a warm (cold) tail event is defined as a set of consecutive warm (cold) tail days (Ballester et al. 2009a, b). Figure 2 depicts the frequency ratio changes for TMEAN warm and cold tail days, where frequency changes are obtained from the average of all land grid points in Europe and shown as a function of the CTL percentile used for the definition of tail days (see x-axis). Similarly, Supplementary Figure 1 displays length ratio changes in TMEAN warm and cold tail events. Also note that similar changes in frequency and length are found for TMAX and TMIN tail days and events (not shown). Discontinuous colored areas represent a measure of model uncertainty in the synthetic scenarios, defined here as one inter-model standard deviation above and below the multi-model mean (e.g., Mathieu et al. 2004; Alexander and Arblaster 2009; Ballester et al. 2009b).

Figure 2 shows that warm tail days become much more frequent in the scenario simulations (see left panels). According to results for TMEAN under B2 (A2) conditions, warm tail days above percentiles P90, P99 and P99.9 will occur about two (2.5), seven (ten) and 25 (45) times more frequently than in CTL, respectively (black lines). Frequency changes in warm tail days are successfully reproduced by both the MS (green) and MSW (red) approaches for all CTL percentiles used for the definition of warm tail days. Nevertheless, the best approach for frequency changes is MSW, with negligible biases within the extreme warm tail. Both the M-B2 and M-A2 (blue) simulations fail to reproduce the frequency changes, showing that a simple shift of annual mean temperatures is not sufficient to explain simulated scenario changes in extremes. Concerning warm tail events, all the approaches are able to reproduce the increase in the length of these events, although the smallest underestimation bias is again found in MSW (Supplementary Figure 1, left panel).

On the other hand, cold tail days are projected to become much less frequent in the future scenarios (see panels on the right in Fig. 2). Under B2 (A2) conditions, cold tail days below percentiles P10, P1 and P0.1 become about three (five), five (20) and 17 (100) times less frequent than in CTL, respectively (in black). Again, MSW (red) is capable of accurately reproducing the expected changes for all percentiles, scenarios

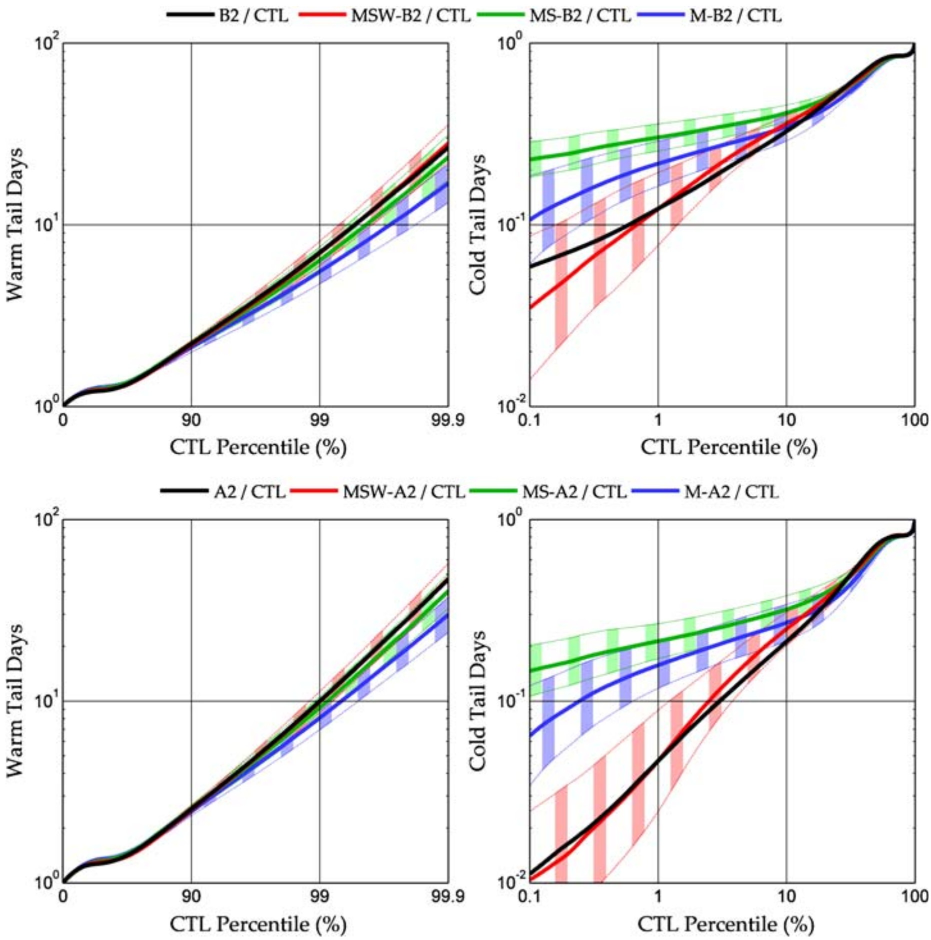

Fig. 2 Ratio changes (scenario/control) in multi-model mean frequency of tail days for detrended daily TMEAN. Warm (cold) tail days in the control or scenario simulations are defined as days above (below) a given percentile of the control simulation (see *x*-axis). Results corresponding to B2 (*top*) and A2 (*bottom*) scenarios (SCE) are shown for M-SCE (*blue*), MS-SCE (*green*), MSW-SCE (*red*) and SCE (*black*). Ratio changes are first averaged for each grid-point in Europe and then for each model. Discontinuous colored areas display a measure of model uncertainty, defined here as one inter-model standard deviation above and below the multi-model mean

and temperature variables, although MSW-B2 slightly overestimates the frequency reduction within the extreme cold tail. Note that both the M (blue) and MS (green) approaches underestimate the frequency reduction of cold tail days, especially in A2. The skewness coefficient also plays a crucial role in the simulation of length changes in cold tail events, since the MSW scheme is the only approach that is able to reproduce the dramatic decrease in the duration of these events (Supplementary Figure 1, panel on the right).

The skill of artificial scenarios in reproducing expected scenario changes in the structure of the PDF is analyzed in Fig. 3 for European average TMEAN (similar results are found for TMAX and TMIN; not shown). For each model and grid-point, detrended daily temperatures are assigned to a percentile within the time series (e.g., P50 for the median of the local temperature time series). Temperature values first assigned to a given percentile are then averaged for grid-points in a region and for the ensemble of models. Scenario anomalies are finally computed as a function of the percentile.

The expected warming in scenarios B2 and A2 is not uniform for percentiles within the warm PDF. The standard deviation and the skewness coefficient are expected to increase in most continental areas (Fig. 1c–f), and therefore percentiles within the extreme warm tail increase more than the central percentiles. Warming differences between the extreme warm tail and central values are thus larger than +1 K for all variables and scenarios (e.g., compare scenario changes of P50 and P99.5 in the black lines of Fig. 3). As a result, estimations from M-B2 and M-A2 (blue) are only correct for some central percentiles, because they reproduce by definition a constant anomaly throughout the PDF, which is equal to the continental mean annual change (Fig. 1a, b). Both the MS (green) and MSW (red) approaches successfully reproduce the expected temperature increase for all percentiles, although the former (latter) scheme underestimates (overestimates) the temperature rise. However, in all cases, temperature biases never exceed ±0.5 K for any warm percentile.

The simulated warming in the cold PDF segment is also larger for the tail than for non-extreme percentiles (e.g., see anomalies of P0.5 and P50 in the black lines of Fig. 3), because the skewness coefficient is expected to increase (Fig. 1e, f). In this case, warming differences within the cold PDF are twice those from the warm PDF

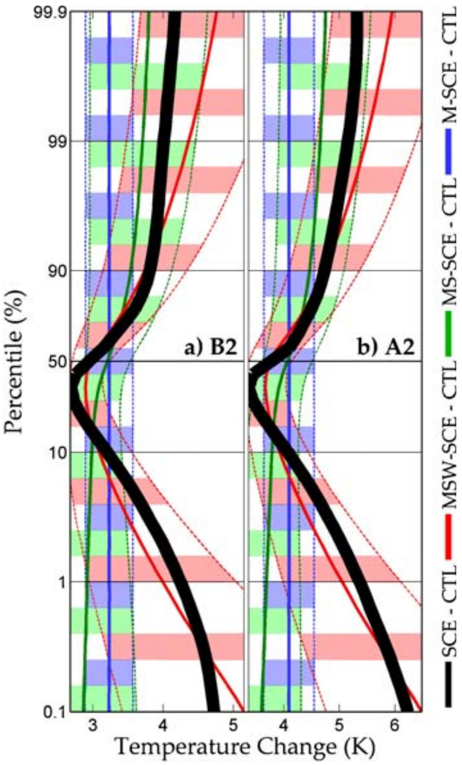

Fig. 3 Multi-model mean anomaly changes (scenario-control) in the structure of the temperature PDF for detrended daily TMEAN (K). For each model and grid-point, temperatures are assigned to a percentile within the time series. Temperatures associated with a given percentile are averaged for grid-points in Europe and for the ensemble of models, and scenario anomalies are then computed as a function of the percentile (see *y*-axis). Discontinuous colored areas display a measure of model uncertainty, defined here as one inter-model standard deviation above and below the multi-model mean

(compare changes in P0.5, P50 and P99.5, black lines in Fig. 3). Therefore, estimations from M-B2 and M-A2 (blue) also fail for non-central percentiles. In addition, the MS approach (green) clearly underestimates the warming in the cold tail, because the standard deviation is expected to increase over most of the continent (mostly in response to an amplification of the seasonal cycle, Fig. 1c, d), and therefore the smallest (largest) warming is simulated for the coldest (warmest) percentiles in this synthetic approach. Under these circumstances, changes in the skewness coefficient play a crucial role in the correct reproduction of changes in the structure of the cold PDF. The MSW approach (red) is indeed able to compensate the negative contribution of the standard deviation change, and biases within the cold PDF are then relatively small for all variables and scenarios.

The results shown in Figs. 2 and 3 and in Supplementary Figure 1 were obtained from averages over all continental grid-points. As seen in Fig. 1, the spatial distribution of scenario changes in the mean, standard deviation and skewness is not uniform, and therefore this spatial structure should be accounted for in the analysis. We thus repeated our calculations for smaller homogeneous regions separately, and the results confirmed the ability of the MSW approach to reproduce the scenario changes, even at the subcontinental scale (see for example Supplementary Figure 2). Similar conclusions were found when the analysis was taken down to the individual grid point level (not shown).

4 Discussion and conclusions

We find that European scenario changes in the tails of the temperature PDF can be successfully reproduced to a first-order approximation after applying simulated changes in the PDF mean, standard deviation and skewness to the control simulation PDF. Intensity anomalies throughout the PDF are shown to be non-trivial and clearly not uniform for the whole range of percentiles, as they are the result of the interaction of changes in multiple processes at several spatiotemporal scales. Therefore, both extreme warm and cold days and events are expected to increase in intensity to a larger degree than central values. Our simple triple transformation successfully deals with this non-uniform behavior. In particular, both the MS and MSW transformations correctly reproduce changes in frequency, length and intensity for the whole range of warm percentiles. Recently, Ballester et al. (2009b) showed that Central Europe heat waves are expected to mostly follow summer mean warming. This is consistent with a combined change in the mean and standard deviation (i.e., to the MS approach), since the increase in standard deviation over this region is mostly a reflection of an increased seasonal cycle (i.e., greater warming in summer than winter (Ballester et al. 2009b)). On the other hand, changes in the skewness coefficient play a crucial role in the simulation of intensity, frequency and length changes in the cold tail. Particularly, the strong intensity increase of cold percentiles is accurately reproduced only by the MSW procedure.

Our results have direct theoretical and practical implications for the predictability of both heat wave and cold spell anomalies in Europe. From a theoretical point of view, our artificial scenarios are transformed only according to anomalies in the mean, standard deviation and/or skewness of the whole PDF. As a general rule, anomalies in these statistics are essentially derived from changes in the portion of variability that corresponds to non-extreme percentiles (i. e., $P1 \leq T \leq P99$), because almost all the variability lies outside the PDF extreme tails. We showed that artificial scenarios only based on changes in these central statistics can reproduce basic changes within both tails. As a result, general changes in the whole PDF (i.e., including changes in both non-extreme and extreme percentiles), rather than specific changes in both extreme tails (i.e., changes within only the tail), can explain most of the magnitude of projected scenario changes in the structure of the tail itself.

From a practical point of view, impact and adaptation studies depending on changes in extremes (McMichael et al. 2006) can be simply based on changes in these three central statistics, for which current climate models are better suited. As an example of application of this finding, projected future time series of daily temperatures can be obtained by transforming observed daily temperature time series as described in this paper, so that they have the same values of these three central statistics as in model simulated future scenarios. This methodology could for example be applied to the study of the expected impact of temperature extremes on infectious diseases (e.g., malaria (Rogers and Randolph 2000)), the incidence of warm and cold-derived illnesses (Haines et al. 2006) or any other aspects concerning socioeconomic organization that are directly linked to the frequency, length and/or intensity of events within the tail of the temperature PDF.

Acknowledgements We acknowledge support from the Catalan Ministry of University and Research, and from the project PANDORA of the Spanish Ministry of Education and Science (reference number CGL2007-63053). Climate simulations have been provided through the PRUDENCE data archive, funded by the EU through contract EVK2-CT2001-00132.

References

Alexander LV, Arblaster JM (2009) Assessing trends in observed and modelled climate extremes over Australia in relation to future projections. Int J Climatol 29:417–435
Ballester J, Douville H, Chauvin F (2009a) Present-day climatology and projected changes of warm and cold days in the CNRM-CM3 global climate model. Clim Dyn 32:35–54
Ballester J, Rodó R, Giorgi F (2009b) Future changes in Central Europe heat waves expected to mostly follow summer mean warming. Clim Dyn. doi:10.1007/s00382-009-0641-5
Christensen JH, Carter TR, Rummukainen M, Amanatidis G (2007) Evaluating the performance and utility of regional climate models: the PRUDENCE project. Clim Change 81:1–6
Giorgi F (2006) Climate change hot-spots. Geophys Res Lett 33:L08707. doi:10.1029/2006GL025734
Giorgi F, Mearns LO (1999) Introduction to special section: regional climate modelling revisited. J Geophys Res 104:6549–6562
Haines A, Kovats RS, Campbell-Lendrum D, Corvalan C (2006) Climate change and human health: impacts, vulnerability, and mitigation. Lancet 9528:2101–2109
IPCC (2007) Climate change 2007: the physical science basis. Cambridge University Press, Cambridge
Mathieu PP, Sutton RT, Dong B, Collins M (2004) Predictability of winter climate over the North Atlantic European Region during ENSO events. J Clim 17:1953–1974
McMichael AJ, Woodruff RE, Hales S (2006) Climate change and human health: present and future risks. Lancet 9513:859–869
Meehl GA, Tebaldi C (2004) More intense, more frequent, and longer lasting heat waves in the 21st century. Science 13:994–997
Parmesan C, Yohe G (2003) A globally coherent fingerprint of climate change impacts across natural systems. Nature 421:37–42
Rodó X, Pascual M, Fuchs G, Faruque ASG (2002) ENSO and cholera: a nonstationary link related to climate change? Proc Natl Acad Sci 99:12901–12906
Rogers DJ, Randolph SE (2000) The global spread of malaria in a future, warmer world. Science 5485:1763–1766